

The Energy Dissipation Rate of Supersonic, Magnetohydrodynamic Turbulence in Molecular Clouds

Mordecai-Mark Mac Low

Max-Planck-Institut für Astronomie, Königstuhl 17, D-69117 Heidelberg, Germany

E-mail: mordecai@mpia-hd.mpg.de

ABSTRACT

Molecular clouds have broad linewidths suggesting turbulent supersonic motions in the clouds. These motions are usually invoked to explain why molecular clouds take much longer than a free-fall time to form stars. It has classically been thought that supersonic hydrodynamical turbulence would dissipate its energy quickly, but that the introduction of strong magnetic fields could maintain these motions. In a previous paper it has been shown, however, that isothermal, compressible, MHD and hydrodynamical turbulence decay at virtually the same rate, requiring that constant driving occur to maintain the observed turbulence. In this paper direct numerical computations of uniformly driven turbulence with the ZEUS astrophysical MHD code are used to derive the absolute value of energy dissipation, which is found to be

$$\dot{E}_{\text{kin}} \simeq -\eta_v m \tilde{k} v_{\text{rms}}^3,$$

with $\eta_v = 0.21/\pi$, where v_{rms} is the root-mean-square velocity in the region, E_{kin} is the total kinetic energy in the region, m is the mass of the region, and \tilde{k} is the driving wavenumber. The ratio of the formal decay time $E_{\text{kin}}/\dot{E}_{\text{kin}}$ of turbulence to the free-fall time of the gas can then be shown to be

$$\tau(\kappa) = \frac{\kappa}{M_{\text{rms}}} \frac{1}{4\pi\eta_v},$$

where M_{rms} is the rms Mach number, and κ is the ratio of the driving wavelength to the Jeans wavelength. It is likely that $\kappa < 1$ is required for turbulence to support gas against gravitational collapse, so the decay time will probably always be far less than the free-fall time in molecular clouds, again showing that turbulence there must be constantly and strongly driven. Finally, the typical decay time constant of the turbulence can be shown to be

$$t_0 \simeq 1.0 \mathcal{L}/v_{\text{rms}},$$

where \mathcal{L} is the driving wavelength.

Subject headings: ISM:Clouds, ISM:Magnetic Fields, Turbulence, ISM:Kinematics and Dynamics, MHD

1. Introduction

Star-forming molecular clouds appear to have lifetimes more than an order of magnitude longer than it would take them to gravitationally collapse in the absence of any support (Blitz & Shu 1980). Typical lifetimes are of order 30 Myr, while the free-fall time

$$t_{\text{ff}} = (3\pi/32G\rho)^{1/2} = (1.2 \times 10^6 \text{ yr})(n/10^3 \text{ cm}^{-3})^{-1/2}, \quad (1)$$

where n is the number density of the cloud and I assume the mean molecular mass $\mu = 3.32 \times 10^{-24}$ g. The gas in molecular clouds also appears to be moving in random directions at supersonic velocities, in a fashion usually described as turbulent. Evidence for this includes molecular emission lines an order of magnitude broader than the thermal linewidth, and the transient, clumpy nature of the clouds (Blitz 1993).

These clumps have been studied in some detail by Stutzki & Güsten (1990), and by Williams, De Geus & Blitz (1994), who showed that regions of enhanced density can be separated out based on their coherent velocity structure. Studies of the formation of photodissociation regions by penetration of UV radiation into the clouds independently lead to the conclusion that the gas is extremely clumpy (Stutzki et al. 1988). Another independent piece of evidence for extreme clumpiness is the studies of dust extinction of background stars through molecular clouds by Lada et al. (1994) and Alves et al. (1998) that show greater variance in extinction in regions with greater average extinction. Models of the chemical abundances in the dense clumps show that they have lifetimes of only a million years or less, much shorter than the lifetimes of the clouds as a whole, but comparable to dynamical and collapse times (Prasad et al. 1991, Bergin et al. 1997).

It has been clear since the discovery of these supersonic motions that supersonic turbulence would decay quickly (e.g. Field 1978), although the common argument that it would decay more quickly than subsonic turbulence due to the extremely dissipative nature of shocks has turned out not to be correct (Mac Low et al. 1998a; hereafter Paper I): rather, supersonic turbulence decays somewhat more slowly than subsonic, incompressible turbulence, though both decay quickly. Magnetic fields have classically been invoked to maintain the observed supersonic motions. The argument has been that the presence of a strong field would transform dissipative shocks to non-dissipative linear magnetohydrodynamic (MHD) waves (Arons & Max 1975, Mouschovias 1975). However, numerical models suggest that the interaction between even mildly non-linear Alfvén waves inevitably generates a spectrum of Alfvén waves with power reaching down to the dissipation scale, however that may be determined (Mac Low et al. 1998b). As a result, compressible magnetohydrodynamic (MHD) turbulence decays at close enough to the same rate as hydrodynamic turbulence as to not be astrophysically distinguishable (Paper I).

Therefore the observed supersonic motions must be driven on timescales short compared to a dynamical time. Luckily, there is no shortage of potential driving mechanisms. In fact,

the problem is not one of finding a plausible driving mechanism, but rather one of choosing from the multiple suspects at hand.

Differential rotation of the galactic disk (Fleck 1981) is attractive as it should apply even to clouds without active star formation. Furthermore, support of clouds against collapse by shear could explain the observation that smaller dwarf galaxies, with lower shear, have larger star-formation regions (Hunter 1998). However, the question arises whether this large-scale driver can actually couple efficiently down to molecular cloud scales. Balbus-Hawley instabilities might play a role here (Balbus & Hawley 1998).

Turbulence driven by gravitational collapse has the attractive feature of being universal: there is no need for any additional outside energy source, as the supporting turbulence is driven by the collapse process itself. Unfortunately, it has been shown by Klessen, Burkert, & Bate (1998) not to work for gas dynamics in a periodic domain. The turbulence dissipates on the same time scale as collapse occurs, without markedly impeding the collapse. The influence of magnetic fields on this problem remains an open question, although the results of Paper I suggest that they will not be important.

Ionizing radiation (McKee 1989, Bertoldi & McKee 1997, Vázquez-Semadeni, Passot & Pouquet 1995), winds, and supernovae from massive stars provide another potential source of energy to support molecular clouds. Here the problem may be that they are too destructive, tending rather to destroy the molecular cloud they act on rather than merely stirring it up. If the clouds can be coupled to a larger-scale interstellar turbulence driven by massive stars, however, perhaps this problem can be avoided.

A final suspect for the driving mechanism is jets and outflows from the more ubiquitous low-mass protostars that should naturally form in any collapsing molecular cloud (McKee 1989, Franco & Cox 1983, Norman & Silk 1980), allowing the attractive possibility of star-formation being a self-limiting process. It has recently become clear that these jets can reach lengths of several parsecs (Bally, Devine, & Alten 1996), implying total energies of order the stellar accretion energy, as suggested by Shu et al. (1988) on theoretical grounds. However, it remains unclear whether space-filling turbulence can be driven by sticking needles into the molecular clouds.

In this paper I consider the most general question required to begin distinguishing among these different models: what is the energy dissipation rate of turbulence uniformly driven at some specified wavelength by an arbitrary forcing field? I consider supersonic turbulence in the presence of magnetic fields with strengths ranging from zero up to somewhat above equipartition with the gas motions. In order to apply my results directly to molecular clouds, I adopt an isothermal equation of state.

2. Computational Technique

To compute the energy dissipation from uniformly driven turbulence I use the astrophysical MHD code ZEUS-3D (Stone & Norman 1992a,b). This is a second-order code using van Leer (1977) advection that evolves magnetic fields using a constrained transport method (Evans & Hawley 1988) modified by upwinding along shear Alfvén characteristics (Hawley & Stone 1995), and that resolves shocks using a Von Neumann type artificial viscosity. It contains no other explicit dissipation or resistivity terms, but structures with size approaching the grid resolution are subject to the usual numerical dissipation.

Using numerical dissipation and artificial viscosity as substitutes for a model of physical dissipation can be justified if the details of the behavior at the dissipation scale can be separated from the larger-scale dynamics of the flow. This assumption appears to be valid in the case of incompressible hydrodynamic turbulence (e.g. Lesieur 1997). In Paper I we studied with some care the question of whether we could also make this assumption in the case of decaying supersonic flow with or without the presence of magnetic fields. We performed resolution studies with grids ranging from 32^3 to 256^3 zones, and found that at resolutions greater than 64^3 zones the power-law in time at which the energy decayed became almost independent of the grid resolution. Because the grid resolution directly determines the scale at which both the numerical dissipation and the artificial viscosity act, this suggests that these scales (or equivalently in the case of the numerical dissipation, its strength) are not important so long as they are separated from the dynamical scale. To further test this assumption, we also compared our results in the hydrodynamic case to computations of the same problem using a smoothed particle hydrodynamics (SPH) code, and found that this very different numerical method again gave very similar answers.

Our resolution studies did reveal that in models with magnetic fields, convergence occurred more slowly in models with initial magnetic energy close to equipartition with the kinetic energy. However, the decay rate monotonically increased with resolution in those models. That is, in models with strong magnetic fields, increased resolution resulted in increased, not decreased, dissipation. Dissipation in these models probably occurs due to the dissipation of short wavelength MHD waves. Higher resolution may better resolve the production of these small wavelength waves by the interaction of non-linear longer wavelength waves with one another.

I perform my computations on a three-dimensional, uniform, Cartesian grid with side $L = 2$, extending from -1 to 1 with periodic boundary conditions in every direction, using an isothermal equation of state, with sound speed chosen to be $c_s = 0.1$. The initial density and, in relevant cases, magnetic field are both initialized uniformly on the grid, with the initial density $\rho_0 = 1$ and the initial field parallel to the z -axis.

To set up a turbulent flow I introduce velocity perturbations in a fashion perhaps too much inspired by models of incompressible turbulence. In those models, a purely solenoidal

flow drawn from a field of Gaussian fluctuations with a power spectrum following a power law $P(k) \propto k^{-q}$ is set up as a reasonable approximation to the distribution of vortices typical of incompressible turbulence, with the index of the power spectrum typically close to the Kolmogorov (1941) value $q = 5/3$. In simulations of supersonic turbulence, a power law with $q = 2$ has been found (e.g. Porter, Pouquet & Woodward 1992, 1994). However, this power spectrum appears to occur for the simple reason that the Fourier transform of a step function is k^{-2} , and Fourier transforms are additive, so the power spectrum of a box full of shocks is also going to be close to k^{-2} . Therefore, setting up a flow drawn from a field of Gaussian fluctuations with $P(k) \propto k^2$, whether only solenoidal (as is done by Padoan & Nordlund 1997), or also including compressible modes, will not be a particularly good approximation to the shock structure typical of supersonic turbulence. Nevertheless, Gaussian fluctuations drawn from a field with power only in a narrow band of wavenumbers around some value k do offer a very simple approximation to driving by mechanisms that act on that scale. Comparing runs with different k then can give some information on how, for example, turbulence driven by large-scale shearing motions might differ from turbulence driven by low mass protostars.

Therefore, I initialize the turbulent flow, as described in Paper I, with velocity perturbations drawn from a Gaussian random field determined by its power distribution \vec{k} in Fourier space, following the usual procedure: for each three-dimensional wavenumber \vec{k} with $k - 1 \leq |\vec{k}| \leq k$ I randomly select an amplitude from a Gaussian distribution around unity and a phase between zero and 2π . I then transform the field back into real space to get a velocity component in each zone, and multiply by the amplitude required to get the desired initial root mean square (rms) velocity. I repeat this for each velocity component independently to get the full velocity field. Thus the dimensionless wavenumber $k = L/\lambda_d$ counts the number of driving wavelengths λ_d in the box.

To drive the turbulence, I then normalize this fixed pattern to produce a set of perturbations $\delta\vec{v}(x, y, z)$, and at every time step add a velocity field $\delta\vec{v}(x, y, z) = A\delta\vec{v}$ to the velocity \vec{v} , with the amplitude A now chosen to maintain constant kinetic energy input rate $\dot{E}_{\text{in}} = \Delta E/\Delta t$. For compressible flow with a time-dependent density distribution, maintaining a constant energy input rate requires solving a quadratic equation in the amplitude A at each time step. For a grid with N zones on a side, each of volume ΔV , the equation for A is

$$\Delta E = \frac{1}{2}\Delta V \sum_{i,j,k=1}^N \rho_{ijk} A \delta\vec{v}_{ijk} \cdot (\vec{v}_{ijk} + A\delta\vec{v}_{ijk}). \quad (2)$$

I take the larger root of this equation to get the value of A .

These computations have no intrinsic scale. To convert to astrophysical units, one must specify mass, length, and time scales or quantities such as density from which these can be derived. One useful set of scales that can be specified is the size of the region considered L' , the mean density ρ' , and the sound speed c'_s . As an example, if we choose $L' = 0.5$ pc,

$c'_s = 0.2 \text{ km s}^{-1}$, and $\rho'_0 = 10^4(2m_H) \text{ g cm}^{-3}$, then the computational time unit t can be converted to seconds as

$$t' = (L'/L)(c_s/c'_s)t = (4 \times 10^{12} \text{ sec}) \left(\frac{L'}{0.5\text{pc}} \right) \left(\frac{c'_s}{0.2 \text{ km s}^{-1}} \right)^{-1} t \quad (3)$$

in our example. Similarly, velocities are scaled with the sound speed

$$v'_{\text{rms}} = (c'_s/c_s)v_{\text{rms}} = (2 \text{ km s}^{-1}) \left(\frac{c'_s}{0.2 \text{ km s}^{-1}} \right) v_{\text{rms}}, \quad (4)$$

energies scale as

$$E' = \frac{\rho'_0}{\rho_0} \left(\frac{L'}{L} \right)^3 \left(\frac{c'_s}{c_s} \right)^2 E = (6 \times 10^{44} \text{ erg}) \left(\frac{L'}{0.5\text{pc}} \right)^3 \left(\frac{c'_s}{0.2 \text{ km s}^{-1}} \right)^2 \left(\frac{n'_0}{10^4 \text{ g cm}^{-3}} \right) E, \quad (5)$$

energy input or dissipation rates scale as

$$\dot{E}' = \frac{\rho'_0}{\rho_0} \left(\frac{L'}{L} \right)^2 \left(\frac{c'_s}{c_s} \right)^3 \dot{E} = (4 \times 10^{-2} L_\odot) \left(\frac{L'}{0.5\text{pc}} \right)^2 \left(\frac{c'_s}{0.2 \text{ km s}^{-1}} \right)^3 \left(\frac{n'_0}{10^4 \text{ g cm}^{-3}} \right) \dot{E}, \quad (6)$$

and so forth.

3. Energy Dissipation

From dimensional arguments, one expects turbulent energy dissipation rates $E'_{\text{kin}} = \eta \mathcal{V}^3 / \mathcal{L}$, where \mathcal{V} and \mathcal{L} are respectively the characteristic velocity and length scale of the turbulent region. However, there are several possible length and velocity scales available. The length scale could, for example, be the size of the box, L , or the typical driving wavelength λ_d , while the velocity scale could be the sound speed c_s , the Alfvén speed v_A , or, as found in one dimension by Gammie & Ostriker (1996), the current mean turbulent velocity v_{rms} . There is also no good theoretical derivation of the value of the constant of proportionality η for strongly compressible turbulence, with or without magnetic fields. The numerical simulations described above are designed to determine η and to decide which of the potential values of \mathcal{V} and \mathcal{L} are correct.

Our resolution studies of models of decaying compressible hydrodynamic and MHD turbulence in Paper I showed that, for the hydrodynamic cases, 128^3 zones captured the decay rate to within a few percent, and even for the MHD cases, this resolution was good to better than 10%. This resolution is also low enough to allow me to do a reasonably sized parameter study on the machines available to me, so I choose it for my standard resolution. I also perform a few runs at 256^3 to check the behavior of my results with increasing resolution, however. In Table 1 I describe the runs at standard resolution discussed in this paper. The model names begin with either H for hydrodynamic or M for MHD, then have

a letter from A to E specifying the level of energy input \dot{E}_{in} , then a number giving the dimensionless wavenumber k chosen for driving, and then, for the MHD models, another number indicating the initial field strength specified by the ratio of the Alfvén speed to the sound speed, v_A/c_s .

To compute the equilibrium values of kinetic energy E_{kin} and root-mean-square (rms) velocity v_{rms} , I took time samples every $2.5 \times 10^{-3}t_s$, where the sound-crossing time $t_s = L/c_s$. After waiting $0.2t_s$ for the turbulence to reach what appeared from the time history to be an approximate steady-state equilibrium, I took the remaining points and computed their mean and variance, typically using several hundred samples. In a few cases, the runs were shorter due to the expense of computing with high Alfvén speeds, though conversely equilibrium was reached more quickly, so I started the averaging at an earlier time to ensure sufficient samples for a meaningful average. The reported quantities have variances under 5% of the mean, except for the kinetic energies of the two hydrodynamic models driven with wavenumber $k = 2$, which had large variances as noted in the table. Driving at large wavenumber in the absence of magnetic fields produces large structures, whose interactions introduce larger fluctuations than usual around the mean.

I find that the best description of my models comes by taking a length scale $\mathcal{L} = \lambda_d$ and a velocity scale $\mathcal{V} = v_{\text{rms}}$. Figure 1(a) shows equilibrium energy dissipation rates for all the models in Table 1, compared to the quantity $kv_{\text{rms}}^3 \sim v_{\text{rms}}^3/\lambda_d$. A fit to the hydrodynamic models HA8 through HE8 gives a relation with slope 1.02. Let us define a dimensionalized wavenumber $\tilde{k} = (2\pi/L)k = 2\pi/\lambda_d$. A very good approximation is then the linear relation

$$\dot{E}_{\text{kin}} \simeq -\eta_v m \tilde{k} v_{\text{rms}}^3, \quad (7)$$

with $\eta_v = 0.21/\pi$, where the assumption is made that in equilibrium $\dot{E}_{\text{kin}} = \dot{E}_{\text{in}}$. The dependence on the mass of the cube m comes strictly from dimensional arguments, as all of the runs in Table 1 have the same mass $m = \rho_0 L^3 = 8$. The strong density fluctuations typical of strongly supersonic turbulence suggest that using the kinetic energy rather than the volume averaged velocity might give a rather different result. In Table 1 I give the ratio $E_{\text{kin}}/0.5mv_{\text{rms}}^2$, showing that in most cases the kinetic energy is 10–15% higher than would be expected for perfectly uncorrelated density and velocity fluctuations. Fitting to the kinetic energies rather than the velocities, as shown in Figure 1(b), the coefficient η_e is about 20% different from the equivalent derived from η_v , and the slope of the relation actually moves slightly away from unity to 1.04. The best linear relation is then

$$\dot{E}_{\text{kin}} = -\eta_e m^{-1/2} \tilde{k} E_{\text{kin}}^{3/2}, \quad (8)$$

with $\eta_e = 0.71/\pi$, where the mass dependence is again included on dimensional grounds. Equation (7) is not only a slightly better fit, but it also brings the other hydrodynamic and MHD models into somewhat better agreement with the relation, so it is mildly preferred.

The MHD models that fit the relation most closely are the strong field cases, with $v_A/c_s = 10$. The weak field cases appear to follow a relation similar to equation (7), but

with values of η_v up to a factor of two higher, as shown in Figure 2. Without further computation, it remains unclear how much of the variation seen among the models is due to the remaining lack of numerical convergence, and how much is real. The higher dissipation seen in the high- β , weak-field cases can be qualitatively explained by noting that weak fields will be more strongly influenced by the flow, generating more dissipative MHD waves. Maron & Goldreich (1999) have used a heavily modified version of ZEUS-3D to compute a relation equivalent to equation (8) for strongly magnetized, trans-Alfvénic turbulence, and find a coefficient equivalent to $\eta_e = 0.23 \pm 0.05$, equal to our value for hydrodynamic turbulence, and agreeing with our result that the strongly magnetized models behave very similarly to the hydrodynamic models.

4. Discussion

4.1. Decay Time vs. Collapse Time

An interesting astrophysical question is whether decaying turbulence can delay gravitational collapse. We can gain insight into this question by examining whether the ratio

$$\tau = t_d/t_{\text{ff}} > 1, \quad (9)$$

where the formal turbulent decay time $t_d = E_{\text{kin}}/\dot{E}_{\text{kin}}$, and the free-fall time t_{ff} for the gas is given by equation (1). Because t_d depends not only on the strength of the turbulence, but also on the driving wavelength, the value of τ also depends on the ratio

$$\kappa = \lambda_d/\lambda_J, \quad (10)$$

where the driving wavelength $\lambda_d = 2\pi/\tilde{k}$, and the Jeans wavelength $\lambda_J = c_s\sqrt{\pi/G\rho_0}$. It has been argued that turbulence cannot support the gas against collapse at wavelengths shorter than the driving wavelength (Bonazzola et al. 1987, 1992; Léorat, Passot, & Pouquet 1992), so that $\kappa \leq 1$. This appears likely, but has not yet been confirmed numerically or observationally. I will address this issue in future work.

Substituting for the values in equation (9), we can write

$$\tau = \frac{E_{\text{kin}}}{\dot{E}_{\text{kin}}} \frac{c_s}{\lambda_J} \sqrt{\frac{32}{3}}. \quad (11)$$

We can now use equation (7) for \dot{E}_{kin} , and, somewhat less accurately, take $E_{\text{kin}} \sim mv_{\text{rms}}^2/2$, noting that this introduces no more than a 20–30% error as shown in Table 1. Substituting and using the definition of κ given in equation (10), I find that the dissipation time scaled in units of the free fall time is

$$\tau(\kappa) = \frac{1}{4\pi\eta_v} \left(\frac{32}{3}\right)^{1/2} \frac{\kappa}{M_{\text{rms}}} \simeq 3.9 \frac{\kappa}{M_{\text{rms}}}, \quad (12)$$

where $M_{\text{rms}} = v_{\text{rms}}/c_s$ is the rms Mach number of the turbulence. In molecular clouds, M_{rms} is typically observed to be of order 10 or higher. If $\kappa < 1$ as argued above, then turbulence will decay long before the cloud collapses and not markedly influence its collapse.

4.2. Comparison to Computations of Decaying Turbulence

In Paper I we examined numerical models of decaying supersonic hydrodynamic and magnetized turbulence and found that its kinetic energy decayed as

$$E_{\text{kin}}(t) = E_{k0}(1 + t/t_0)^{-\alpha} \quad (13)$$

with $0.85 < \alpha < 1.1$, where E_{k0} is the energy at $t = 0$, and t_0 is a time constant that I will discuss below. If we differentiate this, we find

$$\dot{E}_{\text{kin}} = -(\alpha/t_0)E_{k0}^{-1/\alpha}E_{\text{kin}}^{1+1/\alpha}. \quad (14)$$

If we compare this to equation (8), we see that the energy would have to decay with a rate $\alpha = 2$ for consistency, rather than the rate $\alpha \simeq 1$ found in Paper I.

The resolution of this contradiction appears to be that the effective driving wavenumber k in decaying turbulence is not constant but decreases over time. In Figure 3 I show cuts through the density distribution of models C and D of supersonic hydrodynamic decaying turbulence from Paper I showing a visible increase in the typical size of structures as time passes. I show models with both 128^3 and 256^3 resolution to show that the growth in typical size is not dependent on the resolution, although the detailed structure of the models certainly is. To try to demonstrate what such a growth in typical size ought to look like, I show in Figure 4 slices through models HC2, HC4, HC8, HE2, HE4, and HE8 (see Table 1). The MHD case appears more complex. In Figure 5 I show cuts parallel and perpendicular to the magnetic field for the 256^3 decaying model Q from Paper I of supersonic turbulence in the presence of a strong field with initial Alfvén number unity and initial $\beta = 0.005$. The length scale does appear to increase in the structure along the field shown in the parallel slices, but not in the structure across the field shown in the perpendicular slices.

In future work I will try to quantify the growth in typical scales described here, but for now I confine myself to analytically predicting what the time dependence of the effective driving scale \mathcal{L} should be. We can rewrite equation (8) in terms of $\mathcal{L}(t)$ as

$$\dot{E}_{\text{kin}} = 2\pi\eta_e m^{-1/2} \mathcal{L}(t)^{-1} E_{\text{kin}}^{3/2}, \quad (15)$$

and integrate it, assuming that decay from the driven steady state begins at $t = 0$ with an equilibrium energy of E_{k0} to find

$$E_{\text{kin}}(t) = E_{k0} \left[1 + \frac{\pi\eta_e E_{k0}^{1/2}}{m^{1/2}} \int_0^t \frac{dt'}{\mathcal{L}(t')} \right]^{-2}. \quad (16)$$

Now we need to find a functional form for $\mathcal{L}(t)$ that will give a consistent result. A useful choice is

$$\mathcal{L}(t) = \mathcal{L}_0(1 + t/t_0)^{-\alpha/2}, \quad (17)$$

where \mathcal{L}_0 is the driving scale at $t = 0$. Substituting this into equation (16) and integrating, we find

$$E_{\text{kin}}(t) = E_{k0} \left\{ 1 + \frac{2\pi\eta_e E_{k0}^{1/2}}{\alpha m^{1/2}} \frac{t_0}{\mathcal{L}_0} [(1 + t/t_0)^{\alpha/2} - 1] \right\}^{-2}. \quad (18)$$

This expression reduces exactly to the empirical form given by equation (13) if and only if the decay time is given by

$$t_0 = \frac{\alpha m^{1/2} \mathcal{L}_0}{2\pi\eta_e E_{k0}^{1/2}}, \quad (19)$$

thus fixing the value of the decay time t_0 and showing that my measured energy dissipation rates in driven turbulence are consistent with the decay rates measured in Paper I so long as equation (17) for the effective driving scale holds.

If we make the assumption again that $E_{k0} \simeq mv_{\text{rms}}^2/2$, we can see that

$$t_0 = \frac{\alpha}{\eta_e \pi \sqrt{2}} \frac{\mathcal{L}_0}{v_{\text{rms}}}. \quad (20)$$

Remarkably, the coefficient is empirically found to be unity, as η_e was found in the previous section to be almost exactly $(\pi\sqrt{2})^{-1}$, and Paper I showed $\alpha \simeq 1$, so the decay time is just the turbulent crossing time for the driving scale.

Although the decay time t_0 derived here appears to have a different form, it is actually identical to the decay time $t_d = E_{\text{kin}}/\dot{E}_{\text{kin}}$ used in the previous subsection if $\alpha = 1$ and $E_{\text{kin}} = E_{k0}$. This can be seen by substituting for \dot{E}_{kin} from equation (8) and then comparing to t_0 in equation (20) to find $t_0/t_d = \alpha$. Thus, the conclusions drawn there about the ratio of the decay time to the free-fall time remain valid even if the driving scale is time dependent as suggested in this subsection.

I thank E. Zweibel for collaboration on the analysis of decaying turbulence presented in § 4.2, M. Bate, A. Burkert, R. Klessen, C. McKee, Å. Nordlund, M. D. Smith, J. Stone, and E. Vázquez-Semadeni for useful and interesting discussions, and J. Maron and P. Goldreich for permission to quote their result in advance of publication. Computations presented here were performed at the Rechenzentrum Garching of the Max-Planck-Gesellschaft, and at the National Center for Supercomputing Applications (NCSA). ZEUS was used by courtesy of the Laboratory for Computational Astrophysics at the NCSA. This research has made use of NASA's Astrophysics Data System Abstract Service.

REFERENCES

- Alves, J., Lada, C., Lada, E., Kenyon, S., & Phelps, R. 1998, *ApJ*, in press
- Arons, J., & Max, C. E. 1975, *ApJ*, 196, L77
- Balbus, S. A., & Hawley, J. F. 1998, *Rev. Mod. Phys.* 70, 1
- Bally, J., Devine, D., & Alten, V. 1996, *ApJ*, 473, 921
- Bergin, E. A., Goldsmith, P. F., Snell, R. L., & Langer, W. D. 1997, *ApJ*, 482, 285
- Bertoldi, F. B., & McKee, C. F. 1997, *Rev. Mex. Astron. Astrophys. Ser. Conf.*, 6, 195
- Blitz, L. 1993, in *Protostars & Planets III*, eds. E. H. Levy & J. I. Lunine (Tucson: U. of Arizona Press), 125
- Blitz, L., & Shu, F. H. 1980, *ApJ*, 238, 148
- Bonazzola, S., Falgarone, E., Heyvaerts, J., Pérault, M., & Puget, J. L. 1987, *A&A*, 172, 293
- Evans, C. R., & Hawley, J. F. 1988, *ApJ*, 332, 659
- Field, G. B. 1978, in *Protostars & Planets*, ed. T. Gehrels (Tucson: U. of Arizona Press), 243
- Fleck, R. C., Jr. 1981, *ApJ*, 246, L151
- Franco, J., & Cox, D. P. 1983, *ApJ*, 273, 24
- Gammie, C. F., & Ostriker, E. C. 1996, *ApJ*, 466, 814
- Hawley, J. F., & Stone, J. M. 1995, *Computer Phys. Comm.* 89, 127
- Hunter, D. 1998, *PASP*, 109, 937
- Klessen, R. S., Burkert, A., & Bate, M. R. 1998, *ApJ*, 501, L205
- Kolmogorov, A. N. 1941, *Dokl. Akad. Nauk SSSR*, 30, 9
- Lada, C. J., Lada, E. A., Clemens, D. P., & Bally, J. 1994, *ApJ*, 429, 694
- Léorat, J., Passot, T., & Pouquet, A. 1990, *MNRAS*, 243, 293
- Lesieur, M. 1997, *Turbulence in Fluids*, 3rd ed. (Dordrecht: Kluwer), 245
- Mac Low, M.-M., Klessen, R. S., Burkert, A., & Smith, M. D. 1998a, *Phys. Rev. Lett.*, 80, 2754 (Paper I)
- Mac Low, M.-M., Klessen, R. S., Burkert, A., & Smith, M. D. 1998b, in *Interstellar Turbulence*, eds. J. Franco & A. Carraminana (Cambridge: Cambridge U. Press), in press
- Maron, J., & Goldreich, P. 1999, *ApJ*, in preparation
- McKee, C. F. 1989, *ApJ*, 345, 782

- Mouschovias, T. Ch. 1975, Ph.D. thesis, University of California at Berkeley
- Padoan, P., & Nordlund, Å. 1997, ApJ, submitted (astro-ph/970616) (PN)
- Porter, D. H., Pouquet, A., & Woodward, P. R. 1992, Phys. Rev. Lett. 68, 3156
- Porter, D. H., Pouquet, A., & Woodward, P. R. 1994, Phys. Fluids, 6, 2133
- Prasad, S. S., Heere, K. R., & Tarafdar, S. P. 1991, ApJ, 373, 123
- Shu, F. H., Lizano, S., Ruden, S. P., & Najita, J. 1988, ApJ, 328, L19
- Stone, J. M., & Norman, M. L. 1992a, ApJS, 80, 753
- Stone, J. M., & Norman, M. L. 1992b, ApJS, 80, 791
- Norman, C., & Silk, J. 1980, ApJ, 238, 158
- Stutzki, J., & Güsten, R. 1990, ApJ, 356, 513
- Stutzki, J., Stacey, G. J., Genzel, R., Harris, A. I., Jaffe, D. T., & Lugten, J. B. 1988, ApJ, 332, 379
- van Leer, B. 1977, J. Comput. Phys. 23, 276
- Vázquez-Semadeni, E., Passot, T., Pouquet, A. 1995, ApJ, 441, 702
- Williams, J. P., De Geus, E. J., & Blitz, L. 1994, ApJ, 428, 693

Figure Captions

Fig. 1.— Energy dissipation rate for models from Table 1 compared to (a) kv_{rms}^3 or (b) $kE_{\text{kin}}^{3/2}$, where $k = L/\lambda_d$ is the dimensionless wavenumber, and the size of the cube $L = 2$ for all runs. The lines have slope of unity, and are fit to the hydro models HA8 through HE8, yielding the values for the dissipation coefficients $\eta_v = 0.21$ and $\eta_e = 0.71$ (see equations [7] and [8]). Hydrodynamical models are indicated by squares, MHD models by triangles.

Fig. 2.— Dependence of the dissipation coefficient $\eta_v = \dot{E}_{\text{kin}}/(kmv_{\text{rms}}^3)$ on the plasma β , the ratio of thermal to magnetic pressure. Models with weaker fields appear to have as much as a factor two higher dissipation rate.

Fig. 3.— Demonstration that typical size scales appear to increase with time, as suggested by the decay rate. Log of density is shown at times $t/t_s = 0.2, 0.6$ and 1.0 on slices through the decaying supersonic hydrodynamic models C and D described in paper I at standard resolution (128^3) and high resolution (256^3), where t_s is the sound crossing time of our numerical box. Note that each image is scaled to its own maximum and minimum to enhance morphological features.

Fig. 4.— Models showing the appearance of turbulence with different characteristic size scales and driving energy input. Log of density on slices through the hydrodynamic models HC2, HC4, HC8, HE2, HE4, and HE8 (see Table 1) at standard resolution of 128^3 grid points. The value of “drive” given in the figure is \dot{E}_{in} for that model. Note that each image is again scaled to its own maximum and minimum to enhance morphological features.

Fig. 5.— Typical size scales do appear to increase parallel to the field, but not perpendicular to it. Log of density is shown in slices perpendicular and parallel to the magnetic field for the decaying supersonic, MHD model Q from Paper I, with initial Alfvén number unity and initial $\beta = 0.005$. Each image is again scaled to its own maximum and minimum to enhance morphological features.

Table 1. Uniformly Driven Numerical Models

Model	\dot{E}_{in}	k	v_A/c_s	v_{rms}	E_{kin}	$2E_{\text{kin}}/mv_{\text{rms}}^2$
HA8	0.1	8	0	0.191	0.125	0.86
HB8	0.3	8	0	0.272	0.247	0.83
HC2	1	2	0	0.743	2.41*	1.1
HC4	1	4	0	0.530	0.961	0.86
HC8	1	8	0	0.406	0.566	0.86
HD8	3	8	0	0.585	1.21	0.88
HE2	10	2	0	1.50	8.92*	0.99
HE4	10	4	0	1.19	5.43	0.96
HE8	10	8	0	0.872	2.63	0.86
MA4X	0.1	4	10	0.274	0.273	0.91
MA81	0.1	8	1	0.147	0.0763	0.88
MC4X	1	4	10	0.534	0.787	0.69
MC45	1	4	5	0.475	0.754	0.83
MC41	1	4	1	0.467	0.824	0.94
MC85	1	8	5	0.335	0.351	0.78
MC81	1	8	1	0.346	0.425	0.89

Note. — Equilibrium root-mean-square velocities and kinetic energies of numerical models with 128^3 numerical resolution. All quantities have variances less than five percent, except the two starred kinetic energies, which have variances of 20% and 9% respectively.

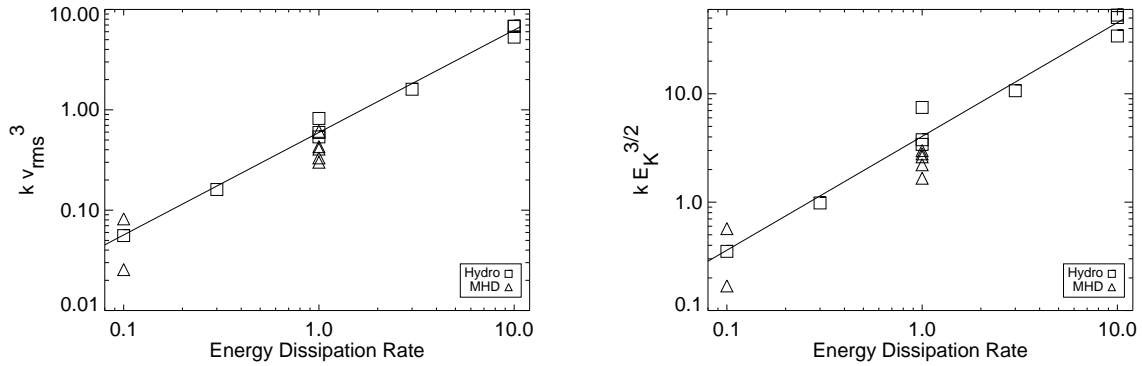


Fig. 1.— Energy dissipation rate for models from Table 1 compared to (a) kv_{rms}^3 or (b) $kE_{\text{kin}}^{3/2}$, where $k = L/\lambda_d$ is the dimensionless wavenumber, and the size of the cube $L = 2$ for all runs. The lines have slope of unity, and are fit to the hydro models HA8 through HE8, yielding the values for the dissipation coefficients $\eta_v = 0.21/\pi$ and $\eta_e = 0.71/\pi$ (see equations [7] and [8]). Hydrodynamical models are indicated by squares, MHD models by triangles.

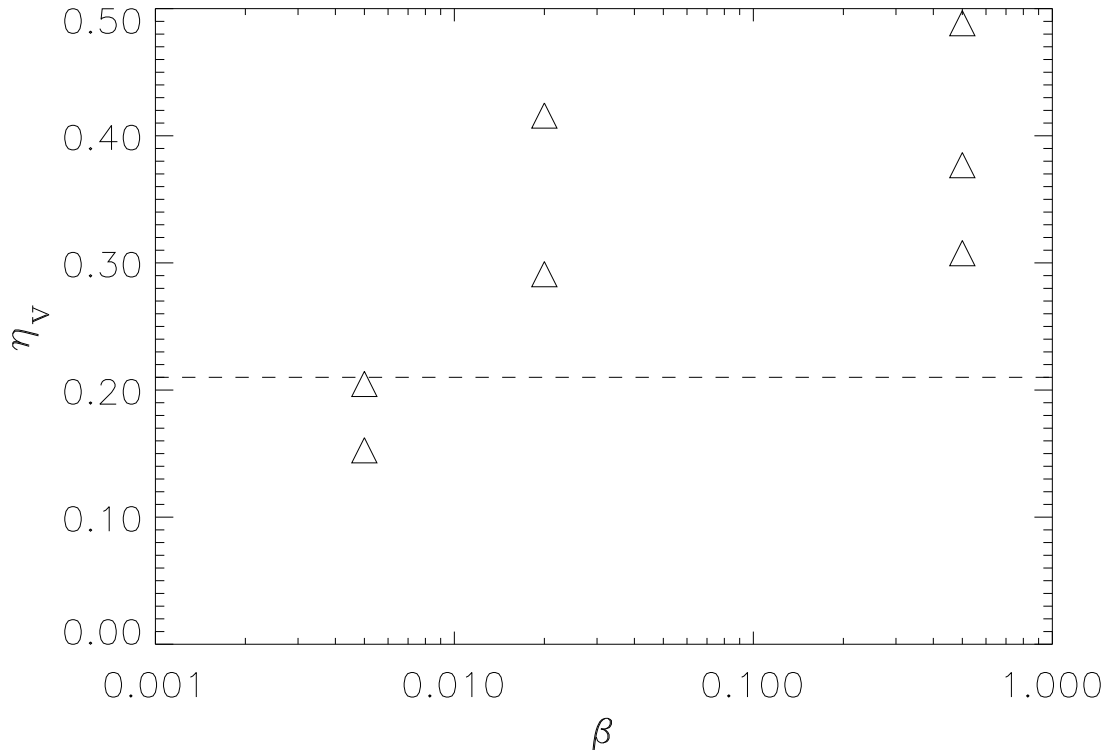


Fig. 2.— Dependence of the dissipation coefficient $\eta_v = \dot{E}_{\text{kin}}/(kmv_{\text{rms}}^3)$ on the plasma β , the ratio of thermal to magnetic pressure. Models with weaker fields appear to have as much as a factor two higher dissipation rate.

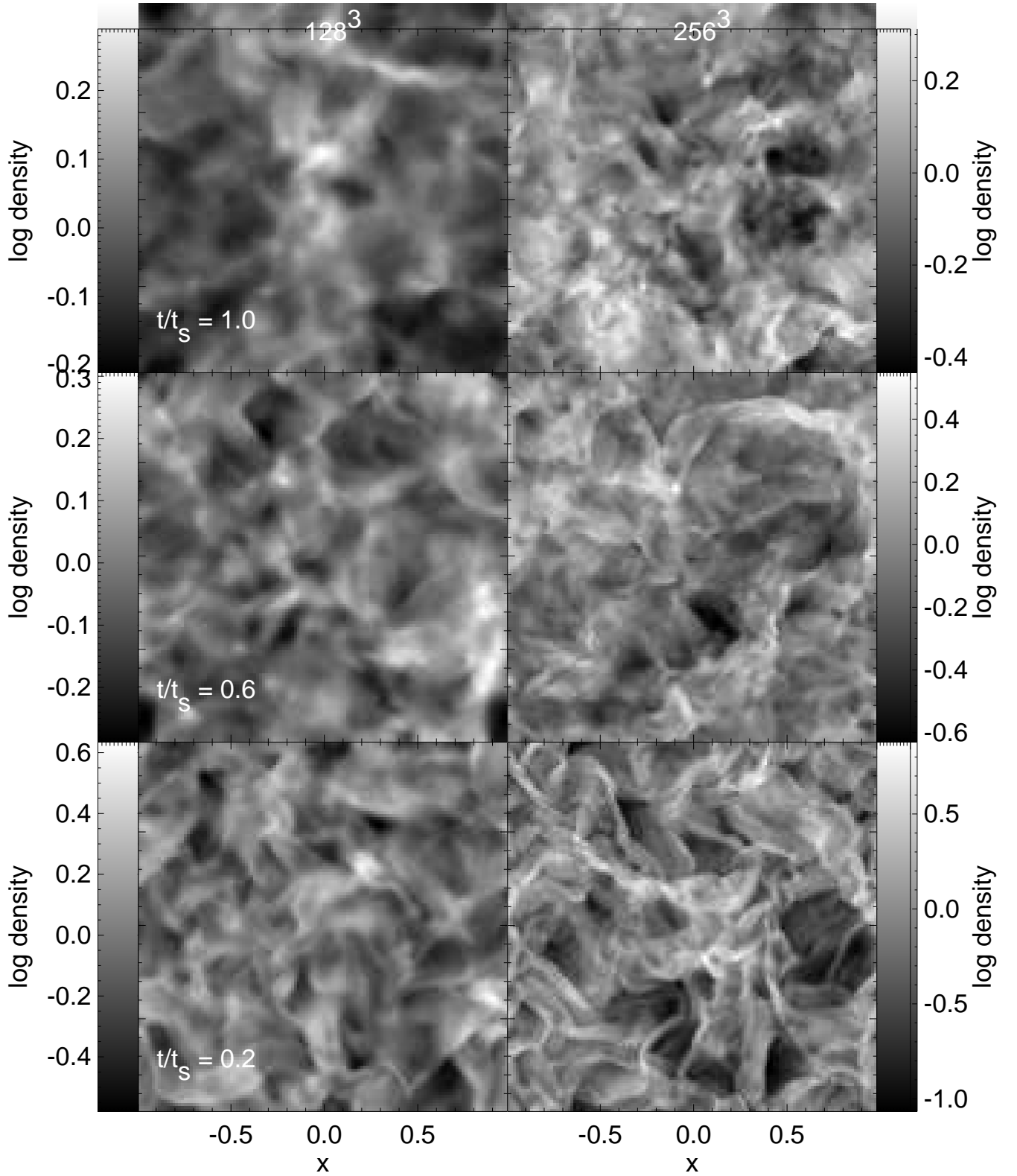


Fig. 3.— Demonstration that typical size scales appear to increase with time, as suggested by the decay rate. Log of density is shown at times $t/t_s = 0.2, 0.6$ and 1.0 on slices through the decaying supersonic hydrodynamic models C and D described in paper I at standard resolution (128^3) and high resolution (256^3), where t_s is the sound crossing time of our numerical box. Note that each image is scaled to its own maximum and minimum to enhance morphological features.

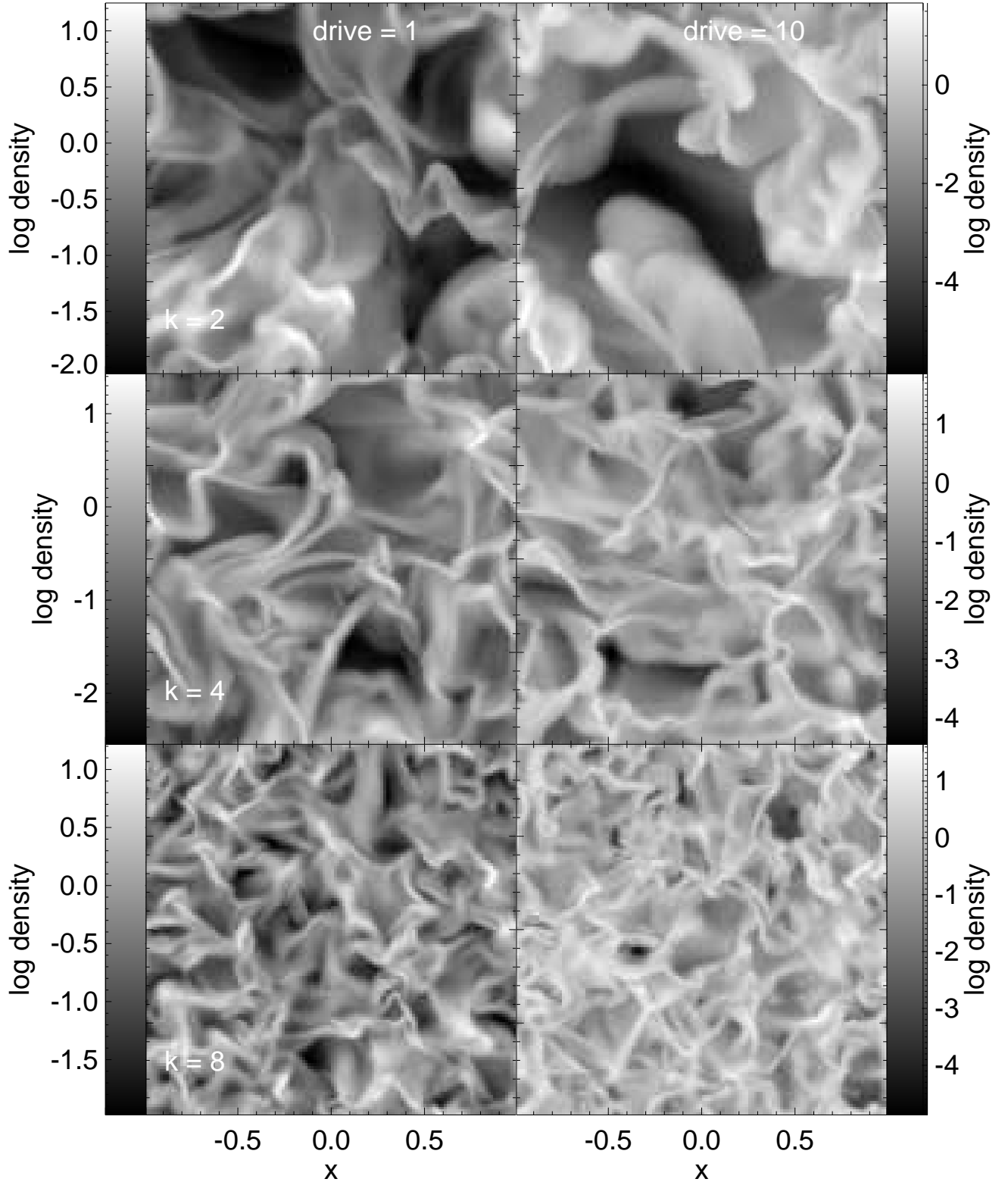


Fig. 4.— Models showing the appearance of turbulence with different characteristic size scales and driving energy input. Log of density on slices through the hydrodynamic models HC2, HC4, HC8, HE2, HE4, and HE8 (see Table 1) at standard resolution of 128^3 grid points. The value of “drive” given in the figure is \dot{E}_{in} for that model. Note that each image is again scaled to its own maximum and minimum to enhance morphological features.

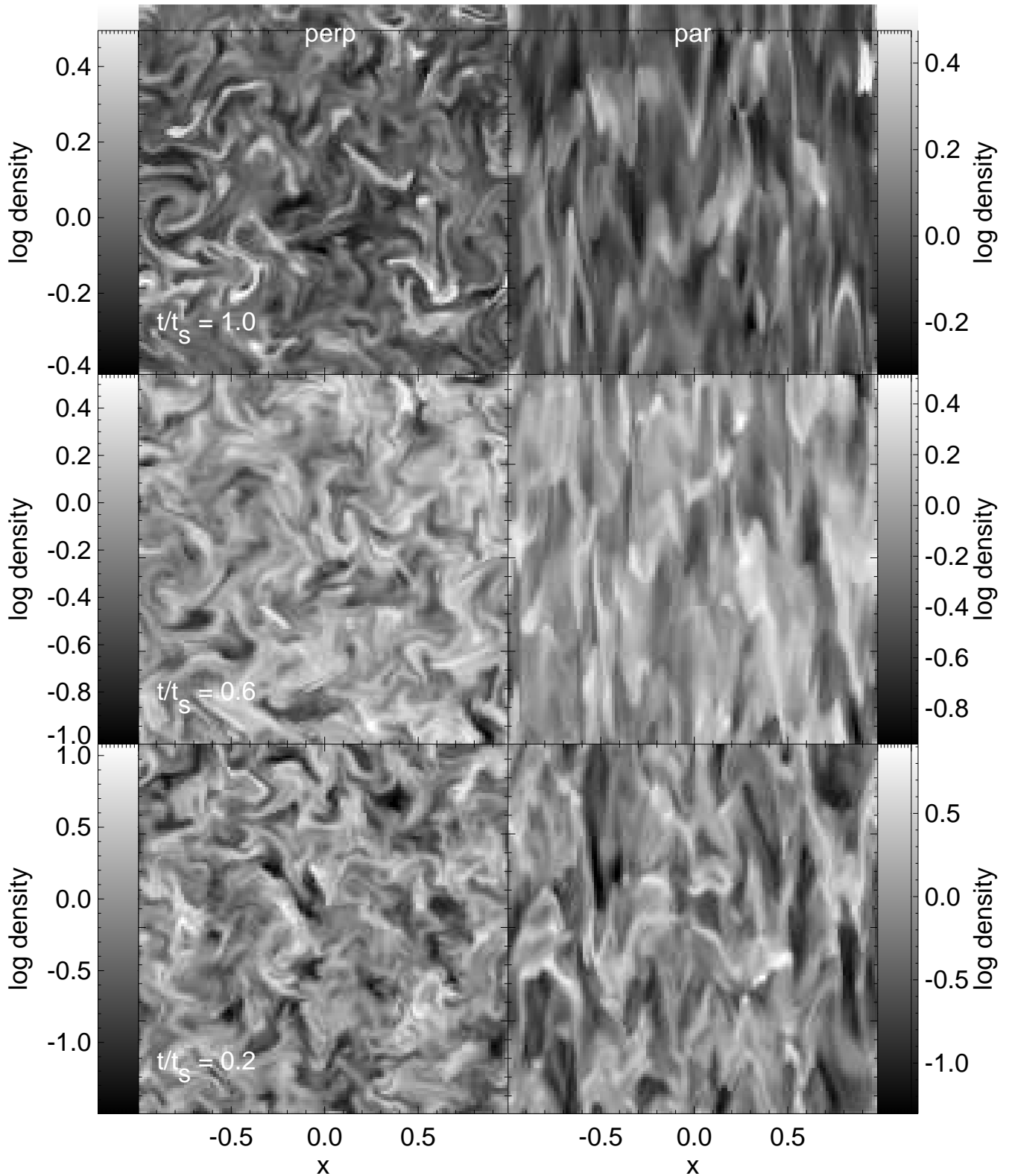


Fig. 5.— Typical size scales do appear to increase parallel to the field, but not perpendicular to it. Log of density is shown in slices perpendicular and parallel to the magnetic field for the decaying supersonic, MHD model Q from Paper I, with initial Alfvén number unity and initial $\beta = 0.005$. Each image is again scaled to its own maximum and minimum to enhance morphological features.